

Synthesis and reactivity of bimetallic iron–rhenium silyl complexes: crystal structures of $[(OC)_3\{(MeO)_3Si\}Fe(\mu-dppm)Re(CO)_4]$ and $[(OC)_3Fe(\mu-Br)(\mu-dppm)Re(CO)_3]$

Michael Knorr^{a,*}, Pierre Braunstein^{a,*}, Antonio Tiripicchio^b, Franco Ugozzoli^b

^a Laboratoire de Chimie de Coordination, Associé au CNRS (URA 0416), Université Louis Pasteur, 4 rue Blaise Pascal, F-67070 Strasbourg Cedex, France

^b Dipartimento di Chimica Generale ed Inorganica, Chimica Analitica, Chimica Fisica, Università di Parma, Centro di Studio per la Strutturistica Diffratometrica del CNR, Viale delle Scienze, I-43100 Parma, Italy

Received 16 April 1996

Abstract

The dppm-bridged heterobimetallic alkoxy-silyl complex $[(OC)_3\{(MeO)_3Si\}Fe(\mu-dppm)Re(CO)_4]$ (**2a**) has been prepared by the reaction of $K[Fe(Si(OMe)_3)(CO)_3(\eta^1-dppm)]$ (**K · 1**) with *fac*- $[Re(\mu-Br)(CO)_3(THF)]_2$ in THF. The Re centre prefers to coordinate an additional CO molecule rather than a lone pair from the potentially bridging $Si(OMe)_3$ ligand. Addition of $BF_3 \cdot xEt_2O$ resulted in replacement of one methoxy group of the $Si(OMe)_3$ ligand by fluorine to afford $[(OC)_3\{(MeO)_2FSi\}Fe(\mu-dppm)Re(CO)_4]$ (**3**). Upon treatment of $[HFe(Si(OMe)_3)(CO)_3(\eta^1-dppm)]$ (**H · 1**) with *fac*- $[Re(\mu-Br)(CO)_3(THF)]_2$ elimination of $HSi(OMe)_3$ occurred, yielding the bromide-bridged complex $[(OC)_3Fe(\mu-Br)(\mu-dppm)Re(CO)_3]$ (**4**). The reactivity of **4** towards phosphines, phosphites, isonitriles and CO has been investigated. Addition of two equivalents of PR_3 to **4** opens the metal–metal bond, yielding $[(OC)_3(R_3P)Fe(\mu-dppm)ReBr(CO)_3(PR_3)]$ (**5**) ($PR_3 = P(OPh)_3, PMePh_2, PMe_2Ph$). The complexes $[(OC)_3(RN \equiv C)Fe(\mu-dppm)ReBr(CO)_3]$ (**8**) ($R = 2,6$ -xylyl, ^tBu) containing a dative metal–metal bond were formed by addition of one equivalent of RNC to a solution of **4**. This dative metal–metal bond is cleaved after addition of a second equivalent of isonitrile to afford $[(OC)_3(RN \equiv C)Fe(\mu-dppm)ReBr(C \equiv NR)(CO)_3]$ (**9**). The related complex $[(OC)_4Fe(\mu-dppm)ReBr(CO)_4]$ (**11**) was obtained by carbonylation of **4** in an autoclave. The corresponding bis(diphenylphosphino)amine-bridged derivative $[(OC)_4Fe(\mu-dppa)ReBr(CO)_4]$ (**13**) was isolated after refluxing a mixture of $[Fe(CO)_4(dppa-P)]$ (**12**) and $[ReBr(CO)_3]$ in toluene. The molecular structures of **2a** and **4** · 0.5CH₂Cl₂ have been determined by X-ray diffraction methods. In the former, the $Re(CO)_4$ and $Fe(CO)_3\{Si(OMe)_3\}$ fragments are linked by a rather long metal–metal bond [$Fe-Re$ 3.013(2) Å] and by a bridging dppm ligand, whereas in **4** the metal–metal bond linking the $Re(CO)_3$ and $Fe(CO)_3$ moieties is much shorter [$Fe-Re$ 2.866(4) Å], being supported by a double bridge: a dppm and a bromine ligand.

1. Introduction

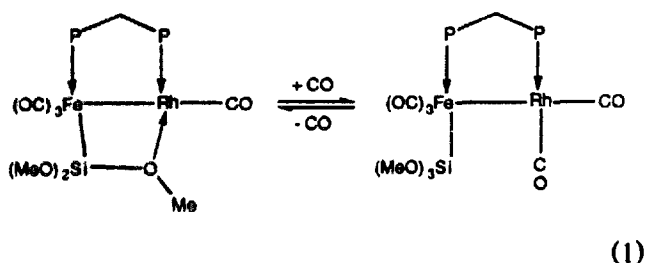
The continuing interest in the preparation and reactivity of heterometallic complexes results from the possibility of investigating (i) cooperative effects between different metal centres which communicate via metal–

metal bonding, (ii) the occurrence of metallo-site selectivity upon reactions with substrate molecules and the comparison with the reactivity of related monometallic complexes, and (iii) possible correlations between unusual bonding modes of coordinated ligands and their activation [1–6]. As part of our studies on silyl-substituted heterobimetallics [7,8], we prepared the Fe–Rh complex $[(OC)_3Fe(\mu-Si(OMe)_2(OMe))(\mu-dppm)Rh(CO)]$ (dppm = $Ph_2PCH_2PPh_2$) by reaction of the potassium metallate $K[Fe(Si(OMe)_3)(CO)_3(\eta^1-dppm)]$ (**K · 1**) with $[Rh(CO)_2(\mu-Cl)]_2$ [9,10]. The most salient feature of this complex was the occurrence of an un-

* Corresponding authors.

[†] Present address: Universität des Saarlandes, Anorganische Chemie, D-66041 Saarbrücken, Germany.

usual $\mu_2\text{-}\eta^2\text{-Si-O}$ bridge that could be opened reversibly under mild conditions by CO to yield the carbonylation product $[(\text{OC})_3\{(\text{MeO})_3\text{Si}\}\text{Fe}(\mu\text{-dppm})\text{Rh}(\text{CO})_2]$ (Eq. (1)).

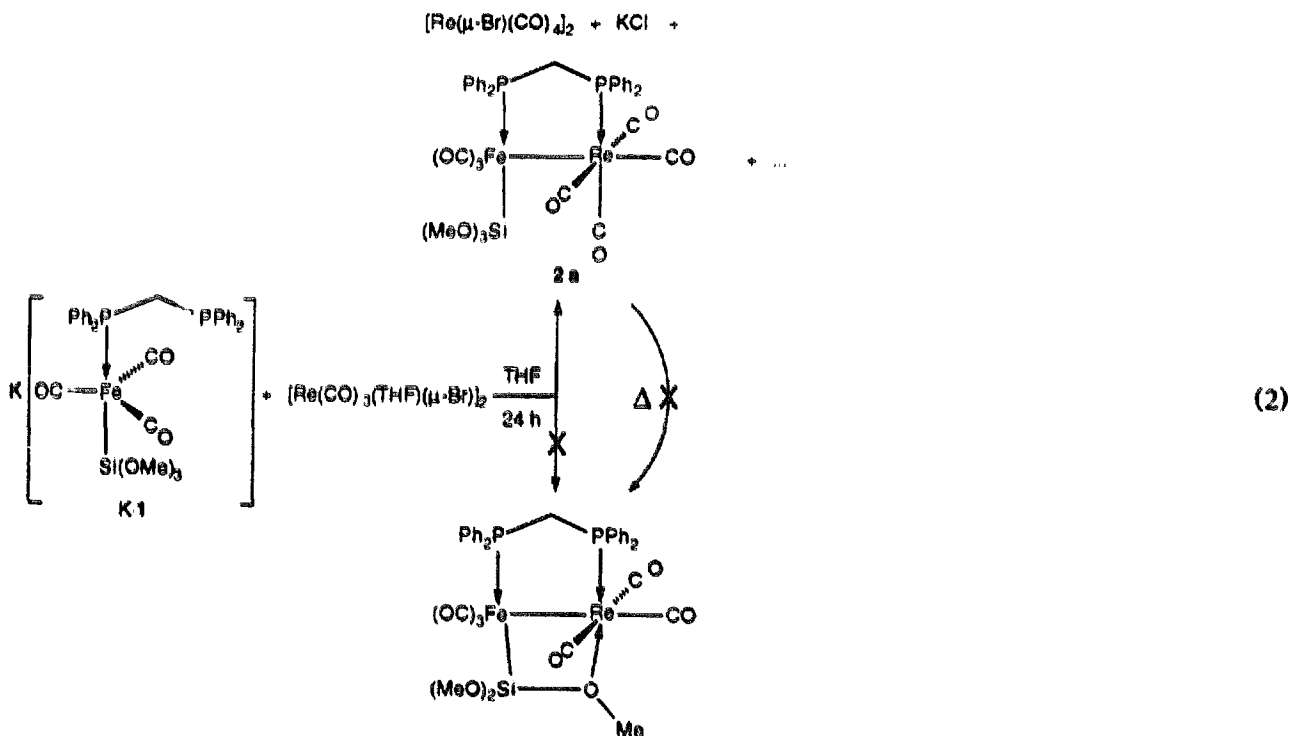


The labile character of the dative oxygen \rightarrow metal interaction offers promising possibilities for the coordination of small molecules to a potentially vacant coordination site. This feature has recently been exploited in related Fe-Pd complexes for the multiple insertion of isonitriles and the sequential insertion of CO and olefins [7].

We therefore set out to prepare related Fe-Re complexes that would display such a masked coordination site and to compare them with other bimetallics containing a similar four-membered cycle.

2. Results and discussion

We reasoned that an Fe-Re complex analogous to $[(\text{OC})_3\text{Fe}(\mu\text{-Si}(\text{OMe})_2(\text{OMe}))(\mu\text{-dppm})\text{Rh}(\text{CO})]$ should be accessible by the reaction of K·1 [11] with *fac*- $[\text{ReBr}(\text{CO})_3(\text{THF})_2]$, which is formed in situ upon dissolving *fac*- $[\text{Re}(\mu\text{-Br})(\text{CO})_3(\text{THF})_2]$ [12] in THF. However, the anticipated product was not observed in the reaction mixture. After separation from $[\text{Re}(\mu\text{-Br})(\text{CO})_4]_2$ and some insoluble material, the reaction mixture was examined by ^{31}P NMR spectroscopy which showed the presence of **2a** as the major component, together with small amounts of another product (Eq. (2)).



The $^{31}\text{P}\{^1\text{H}\}$ NMR spectrum of **2a** displays a doublet at δ 59.6 for the P nucleus on iron and another doublet for the P nucleus on rhenium at δ 1.0 with a typical $^{2+3}J(\text{P-P})$ coupling of 92 Hz. The second, as yet uncharacterized, compound gave rise to an AX pattern centred at δ 61.9 and δ 11.1 (d, $^{2+3}J(\text{P-P}) = 108$ Hz).

Pure **2a** was obtained in moderate yield after extraction with Et_2O in the form of stable yellow crystals.

A view of the solid-state structure of **2a**, determined by X-ray diffraction, is shown in Fig. 1, together with the atomic numbering scheme. Selected bond distances and angles are given in Table 1.

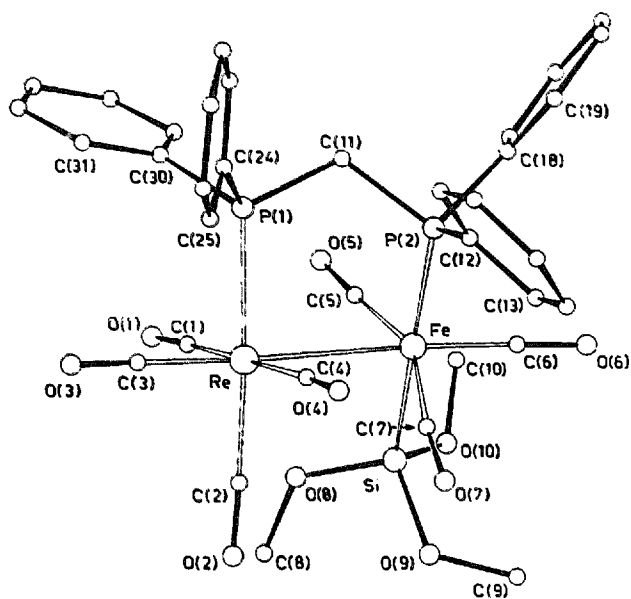


Fig. 1. View of the molecular structure of the complex $[(OC)_3((MeO)_3Si)Fe(\mu-dppm)Re(CO)_4]$ (**2a**) together with the atomic numbering scheme.

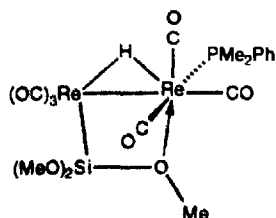
The $Re(CO)_4$ and $Fe(CO)_3(Si(OMe)_3)$ fragments are linked by a metal–metal bond [Fe–Re 3.013(2) Å] and by a bridging dppm molecule. The octahedral environment of the Fe atom is determined by the Re atom and three carbon atoms from terminal carbonyl groups in the equatorial sites, by the P(2) atom from dppm [Fe–P(2) 2.241(2) Å] and by the Si atom of the trimethoxysilyl ligand [Fe–Si 2.300(2) Å] in the apical positions. The octahedral coordination around the Re atom involves the Fe atom and three carbon atoms from terminal carbonyl groups in the equatorial positions, the P(1) atom from the dppm ligand [Re–P(1) 2.435(2) Å] and one carbon atom from a terminal carbonyl group in the apical positions. The torsion angle ReP(1)P(2)Fe amounts to 25.2(1)° and the corresponding twist between the two metal coordination polyhedra is also reflected in the dihedral angle of 28.8(2)° between the mean planes ReC(1)C(3)C(4) and FeC(5)C(6)C(7). The Fe–Re distance appears to be the longest reported so far for complexes containing Fe–Re bonds (usually observed in the range 2.671–2.893 Å, from Cambridge Crystallographic Data Centre) and is also much longer than that found in **4** (see below). In the complexes $(\eta^5-C_5H_5)(OC)_2Fe-Re(CO)_5$ and $(\eta^5-C_5H_5)(OC)_2Fe-Re(CO)_4(CN^tBu)$, the values of the unbridged metal–metal separations are 2.888(1) and 2.893(1) Å respectively [4,13]. As pointed out previously there is no bonding interaction in **2a** between the alkoxysilyl ligand and the Re atom, the shortest contact between the Re atom and oxygen atoms being 3.692(4) Å with O(8).

The somewhat unexpected preference of the Re centre for CO coordination over intramolecular formation of a $\mu_2-\eta^2-Si-O$ bridge is such that heating **2a** in refluxing THF or heptane did not lead to decarbonylation and **2a** was recovered unchanged. Addition of trimethylamine oxide caused only slow decomposition. The complex was also inert towards addition of one equivalent of $tBuNC$ in refluxing CH_2Cl_2 for 1 h. The fourth carbonyl ligand on Re must arise from partial decomposition. We have already communicated the preparation of the derivative $[(OC)_3((Me_3SiO)_2-MeSi)Fe(\mu-dppm)Re(CO)_4]$ (**2b**), in which the $Si(OMe)_3$ group is replaced by a siloxyl unit [14]. Consistent with the present findings, no $\mu_2-\eta^2-Si-O$ bridge was found in **2b**, although we have recently demonstrated their occurrence in related Fe–Pd complexes [15]. We can provide no satisfactory explanation as to why, in these cases, no $\mu_2-\eta^2-Si-O$ bridge was formed, in spite of the known oxophilic character of rhenium, whereas this bonding mode has been observed by us in many other Fe–M complexes (M = Pd, Pt, Rh, Ag). In the complex $[(OC)_4Fe(\mu-C(Me)O)Re(CO)_4]$, the acyl ligand bridges the two metals via a dative interaction between its oxygen and the rhenium centre [16]. Moreover, examples of dirhenium complexes of the type $[(OC)_3Re(\mu_2-\eta^2-Si(OMe)_2(O^Me))(\mu-H)Re(CO)_3L]$ (L = CO, PMe_2-

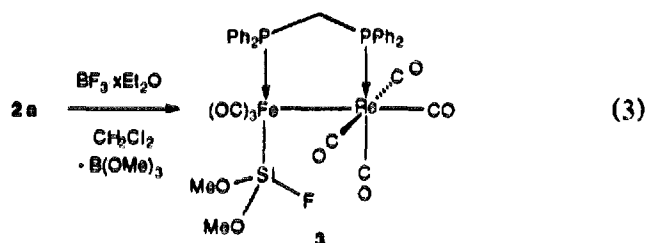
Table 1
Selected bond distances (Å) and angles (°) in the complex **2a**

Re–Fe	3.013(2)	Si–O(8)	1.613(5)
Re–P(1)	2.435(2)	Si–O(9)	1.658(4)
Re–C(1)	1.988(5)	Si–O(10)	1.611(3)
Re–C(2)	1.942(6)	C(1)–O(1)	1.115(6)
Re–C(3)	1.868(6)	C(2)–O(2)	1.151(8)
Re–C(4)	2.013(5)	C(3)–O(3)	1.176(7)
Fe–P(2)	2.241(2)	C(4)–O(4)	1.100(6)
Fe–Si	2.300(2)	C(5)–O(5)	1.146(5)
Fe–C(5)	1.760(4)	C(6)–O(6)	1.160(8)
Fe–C(6)	1.743(6)	C(7)–O(7)	1.144(6)
Fe–C(7)	1.786(5)		
Fe–Re–P(1)	89.5(1)	P(2)–Fe–C(5)	93.6(2)
Fe–Re–C(1)	88.6(2)	P(2)–Fe–C(6)	91.2(2)
Fe–Re–C(2)	92.4(2)	P(2)–Fe–C(7)	102.5(2)
Fe–Re–C(4)	88.9(2)	Si–Fe–C(5)	80.9(2)
P(1)–Re–C(1)	89.4(2)	Si–Fe–C(6)	85.4(2)
P(1)–Re–C(3)	87.8(2)	Si–Fe–C(7)	84.3(2)
P(1)–Re–C(4)	91.5(2)	C(5)–Fe–C(7)	103.3(3)
C(1)–Re–C(2)	88.3(2)	C(6)–Fe–C(7)	98.4(3)
C(1)–Re–C(3)	89.7(2)	Re–C(1)–O(1)	176.5(4)
C(2)–Re–C(3)	90.1(2)	Re–C(2)–O(2)	177.3(5)
C(2)–Re–C(4)	90.9(2)	Re–C(3)–O(3)	179.6(5)
C(3)–Re–C(4)	92.7(2)	Re–C(4)–O(4)	176.5(5)
Re–Fe–P(2)	87.3(1)	Fe–C(5)–O(5)	176.1(4)
Re–Fe–Si	96.8(1)	Fe–C(6)–O(6)	177.8(5)
Re–Fe–C(5)	84.4(2)	Fe–C(7)–O(7)	172.1(5)
Re–Fe–C(7)	74.5(2)		

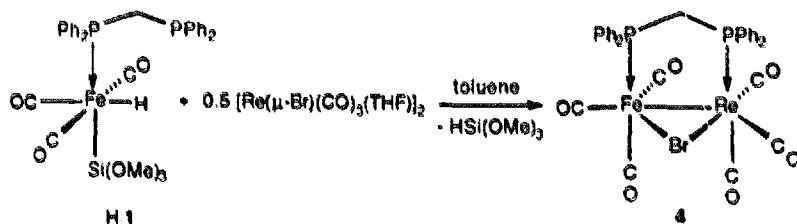
Ph) which display this type of interaction have recently been structurally characterized by Adams et al. [17].



Reaction of **2a** with one equivalent of $\text{BF}_3 \cdot x\text{Et}_2\text{O}$ led to replacement of only one methoxy group of the $\text{Si}(\text{OMe})_3$ ligand by fluorine and afforded the stable complex $[(\text{OC})_3\{(\text{MeO})_2\text{FSi}\}\text{Fe}(\mu\text{-dppm})\text{Re}(\text{CO})_4]$ (**3**) (Eq. (3)).



Diagnostic for this monofluorination reaction is the ^{31}P NMR spectrum of **3**, which exhibits a doublet at δ 0.5 for the rhenium-bound phosphorus and a doublet of doublets at δ 59.0 for the iron-bound phosphorus due to a $^2+^3J(\text{P}=\text{P})$ coupling of 90 Hz and a $^1J(\text{P}=\text{F})$ coupling of 18 Hz. The same $^1J(\text{P}=\text{F})$ coupling of 18 Hz was also found in the ^{19}F NMR spectrum where the doublet at δ = 96.5 was in addition flanked by ^{29}Si satellites ($^1J(\text{Si}=\text{F}) = 365$ Hz). Because of a $^1J(\text{C}=\text{F})$ coupling of 4 Hz, the $^{13}\text{C}\{^1\text{H}\}$ resonances of the methoxy groups are split



A view of the molecular structure of **4**, determined by X-ray diffraction, is shown in Fig. 2, together with the atomic numbering scheme; selected bond distances and angles are given in Table 2.

In the crystals, CH_2Cl_2 molecules of solvation are present. The $\text{Re}(\text{CO})_3$ and $\text{Fe}(\text{CO})_3$ fragments are linked by a metal–metal bond [$\text{Fe}=\text{Re}$ 2.866(4) Å] and by a double bridge: a Br atom [$\text{Fe}=\text{Br}$ 2.472(5) Å and $\text{Re}=\text{Br}$

into a doublet at δ 51.0. As in **2a** the resonances for the carbonyl ligands on iron, in the 216–211 ppm range, are distinctly separated from those for the carbonyls on rhenium, which are found between 193 and 185 ppm (see Section 3). Note that upon reaction of $[(\text{OC})_3\{(\text{MeO})_3\text{Si}\}\text{Fe}(\mu\text{-dppm})\text{Pt}(\text{H})(\text{PPh}_3)]$ with $\text{BF}_3 \cdot x\text{Et}_2\text{O}$ under similar conditions, complete substitution of the methoxy groups occurred to yield the SiF_3 derivative [18]. In the presence of an excess of $\text{BF}_3 \cdot x\text{Et}_2\text{O}$, **3** slowly underwent further F/OMe exchange as evidenced by ^{31}P NMR and IR monitoring. The isolation of a pure product failed, however, due to competing reactions, possibly involving rupture of the metal–silicon bond.

Another access to silyl-substituted heterobimetallics consists in the oxidative addition of the $\text{Fe}=\text{H}$ function of **1** across a low valent metal centre. We have previously used this approach to prepare a range of $\text{Si}(\text{OR})_3$ -substituted complexes containing Pd, Pt, Rh or Ru [10,19,20]. When equimolar amounts of **1** and *fac*- $[\text{Re}(\mu\text{-Br})(\text{CO})_3(\text{THF})_2]_2$ were mixed in toluene (Eq. (4)), a rapid reaction occurred and an orange–yellow product precipitated, which was identified by means of elemental analyses, spectroscopic data and X-ray diffraction as the bromide-bridged complex $[(\text{OC})_3\text{Fe}(\mu\text{-Br})(\mu\text{-dppm})\text{Re}(\text{CO})_3]$ (**4**). That elimination of $\text{HSi}(\text{OMe})_3$ had occurred was confirmed by ^1H NMR monitoring of the reaction in an NMR tube, using C_6D_6 as solvent. No evidence for an intermediate hydrido species could be obtained. Owing to the dissymmetry of this A-frame type molecule, there are now two distinct resonances for the methylene protons of the dppm bridge (ABXY-type pattern; X, Y = P), whereas in the silyl-substituted derivatives **2a** and **3**, triplet patterns (overlapping doublets of doublets) were observed. The $^{31}\text{P}\{^1\text{H}\}$ NMR spectrum of **4** displays a doublet at δ 57.2 for the P nucleus on iron and a second doublet for the P nucleus on rhenium at δ 10.4 ($^2+^3J(\text{P}=\text{P}) = 80$ Hz).

2.628(5) Å] and a dppm molecule. The octahedral environment about the Fe atom is determined by the Re atom, the Br atom and two carbon atoms from carbonyl groups in the equatorial positions, by the P(2) atom from dppm [$\text{Fe}=\text{P}(2)$ 2.275(5) Å] and by a carbon atom from a carbonyl group in the axial position. The octahedral coordination of the Re atom involves the Fe atom, the Br atom and two carbon atoms from carbonyl

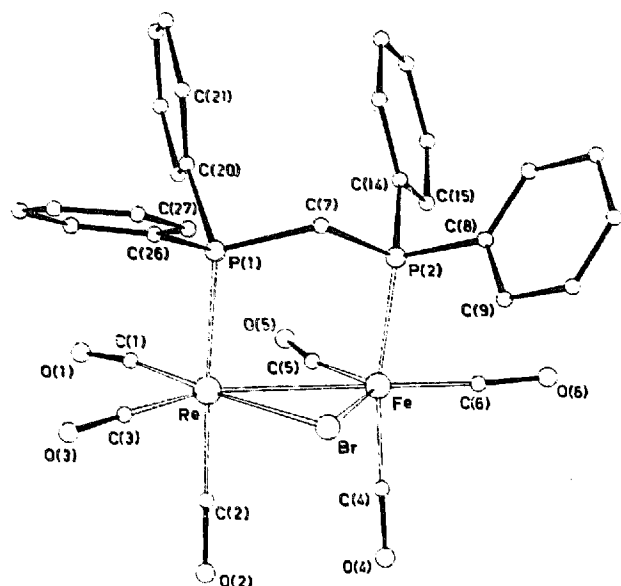


Fig. 2. View of the molecular structure of the complex $[(OC)_3Fe(\mu-Br)(\mu-dppm)Re(CO)_3]$ (**4**) together with the atomic numbering scheme.

groups in the equatorial positions, the P(1) atom from the dppm ligand [Re–P(1) 2.468(5) Å] and one carbon atom from a carbonyl group in the axial positions. Of the six carbonyls, one is semi-bridging the two metal atoms [Re–C(5) 2.654(16) Å; Fe–C(5)–O(5) 167(2)°]. This feature is probably absent in solution, since the IR data in CH_2Cl_2 only indicate terminal carbonyls. The Fe–Re distance is much shorter than in **4**, and is comparable with that found in the acyl-bridged com-

Table 2
Selected bond distances (Å) and angles (°) in the complex **4**

Re–Fe	2.866(4)	Fe–C(5)	1.75(3)
Re–Br	2.628(5)	Fe–C(6)	1.75(2)
Re–P(1)	2.468(5)	C(1)–O(1)	1.17(4)
Re–C(1)	1.88(2)	C(2)–O(2)	1.22(2)
Re–C(2)	1.87(2)	C(3)–O(3)	1.18(2)
Re–C(3)	1.87(2)	C(4)–O(4)	1.18(2)
Fe–Br	2.472(5)	C(5)–O(5)	1.16(3)
Fe–P(2)	2.275(5)	C(6)–O(6)	1.18(2)
Fe–C(4)	1.75(2)		
Fe–Re–P(1)	89.2(1)	Br–Fe–P(2)	90.1(2)
Fe–Re–Br	53.3(1)	Br–Fe–C(4)	90.7(6)
Fe–Re–C(2)	88.8(5)	Br–Fe–C(5)	123.5(7)
Fe–Re–C(4)	122.3(5)	P(2)–Fe–C(5)	95.1(6)
Br–Re–P(1)	87.4(2)	P(2)–Fe–C(6)	87.0(6)
Br–Re–C(2)	88.7(7)	C(4)–Fe–C(5)	92.9(9)
Br–Re–C(3)	98.0(8)	C(4)–Fe–C(6)	84.3(8)
P(1)–Re–C(1)	93.0(5)	C(5)–Fe–C(6)	110.1(8)
P(1)–Re–C(3)	92.6(7)	Re–Br–Fe	68.3(1)
C(1)–Re–C(2)	91.0(9)	Re–C(1)–O(1)	173(2)
C(1)–Re–C(3)	86.3(9)	Re–C(2)–O(2)	178(2)
C(2)–Re–C(3)	87.6(9)	Re–C(3)–O(3)	177(2)
Re–Fe–P(2)	95.3(2)	Fe–C(4)–O(4)	178(2)
Re–Fe–Br	58.4(1)	Fe–C(5)–O(5)	167(2)
Re–Fe–C(4)	93.9(5)	Fe–C(6)–O(6)	176(2)
Re–Fe–C(5)	65.0(5)		

plexes $[(OC)_4Fe(\mu-C(O)R)Re(CO)_3]$ (R = Ph, 2.841(1) Å; R = Me, 2.861(1) Å) [16] or the μ -alkylidene complex $[(OC)_4Fe(\mu-C(H)Ph)ReCp(CO)_2]$ [2.7581(8) Å] [21].

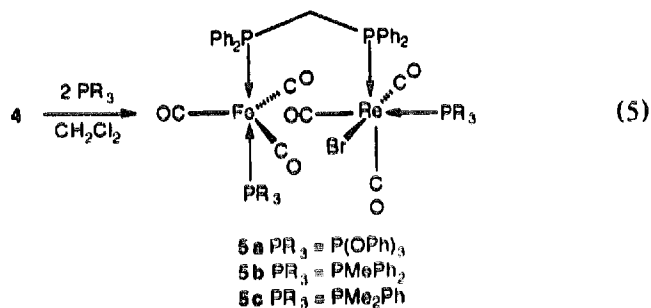
2.1. Reactivity studies on $[(OC)_3Fe(\mu-Br)(\mu-dppm)Re(CO)_3]$ (**4**)

2.1.1. Attempted reaction with DMAD

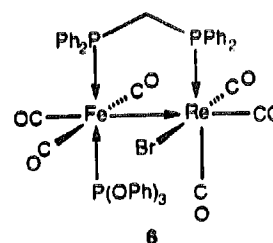
No reaction took place when two equivalents of the activated alkyne $MeO(O)CC\equiv CC(O)OMe$ (DMAD) were added to a CH_2Cl_2 solution of **4**, even under prolonged stirring. This contrasts with the recent finding of Adams and coworker [22] who investigated the insertion of DMAD into the metal–metal bond of $[Cp(OC)_2Fe-Re(CO)_5]$ and isolated the dimetallated olefin complex $[Cp(CO)_2Fe(\mu-(Z)-MeO(O)CC=CC(O)OMe)Re(CO)_4]$.

2.1.2. Reactions with phosphorus donors

Upon addition of two equivalents of PPh_3 or $Ph_2PCH_2C(O)Ph$ [23] to a CH_2Cl_2 solution of **4**, no reaction took place. However, PMe_2Ph , $PMePh_2$ or $P(Ph)_3$ reacted rapidly under cleavage of the metal–metal bond to afford complexes **5a–c** in nearly quantitative spectroscopic yield (Eq. (5)).



Upon addition of only one equivalent of $PMePh_2$ or PMe_2Ph , only **5b** or **5c** respectively and 50% of the starting material were recovered. In the case of $P(OPh)_3$, the intermediate **6** could be detected by ^{31}P NMR monitoring before its transformation to **5a**.



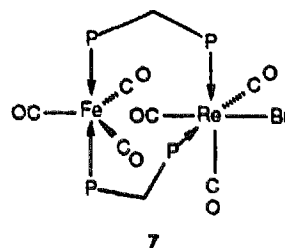
Initial attack of the phosphite on the iron centre was unambiguously established by the observation in the

$^{31}\text{P}\{^1\text{H}\}$ NMR spectrum of a doublet of doublets at δ 155.4 with a strong *trans*-coupling of 198 Hz with the iron-bound dppm-phosphorus and a smaller coupling of 10 Hz with the dppm-phosphorus on Re. The same strong *trans*-coupling was obviously also found in the resonance of the iron-bound dppm-phosphorus at δ 57.8, which was further coupled with the dppm-phosphorus on Re by 84 Hz. This latter phosphorus gives rise to a doublet of doublets at δ 6.9, with couplings of 10 and 84 Hz. We therefore suggest for **6** the ligand arrangement depicted which was also observed in the isonitrile-substituted complexes **8** (see below). A formal $\text{Fe}(0) \rightarrow \text{Re}(I)$ dative bond leads to an 18 electron count for each metal.

The cleavage of the metal-metal bond in **5** and the ligand arrangement about the two metal centres were deduced by combined spectroscopic methods as exemplified for **5b**. The ^{31}P NMR spectrum is first order and consists of two triplets and two doublets, which are all accidentally coupled by 32 Hz. The first triplet and doublet at δ 77.1 and 65.4 respectively are assigned to the dppm-phosphorus and the PMePh_2 on iron, whereas the higher field signals at δ -2.6 and -19.1 are assigned to the rhenium-bound dppm and PMePh_2 respectively. A similar *trans*-coupling of 32 Hz has also been observed in the mononuclear complex *trans*- $[\text{Fe}(\text{CO})_3(\text{PPh}_3)(\text{dppm}-P)]$ [10]. As in the IR spectrum of the latter compound, the three equatorial carbonyls on iron give rise to a strong absorption at 1885 cm^{-1} with an additional shoulder at 1877 cm^{-1} . This shoulder may be due to a lowering of the symmetry about the iron fragment (splitting of the E-mode), since more

symmetric species like *trans*- $[\text{Fe}(\text{CO})_3(\text{PPh}_3)_2]$ show only one strong E-mode vibration at 1886 cm^{-1} . The pattern and the position of the three Re-CO absorptions (2033 vs, 1952 s, 1905 s) are very similar to those reported for mononuclear complexes of the type *fac*- $[\text{Re}(\text{X})(\text{CO})_3(\text{PR}_3)_2]$ [24,25] or for the recently prepared trinuclear complex *fac*- $[\text{Re}(\text{Br})(\text{CO})_3\{(\mu\text{-dppm})\text{Mn}(\eta\text{-C}_5\text{H}_4\text{Me})(\text{CO})_2\}_2]$ [26]. In the far IR spectrum of **5a** the Re-Br stretch is observed at 197 cm^{-1} , typical for terminal Re-Br vibrations.

When dppm was added to a CH_2Cl_2 solution of **4**, complex **7** was formed as the main product, as evidenced by ^{31}P NMR spectroscopy. The spectrum exhibits a typical AA'XX' pattern with $N = 74\text{ Hz}$ ($N = |^2J(\text{P}_A\text{P}_X) + ^4J(\text{P}_A\text{P}_X)|$) at δ 75.0 for the dppm-phosphorus on Fe and at δ -24.9 for the dppm-phosphorus on Re.

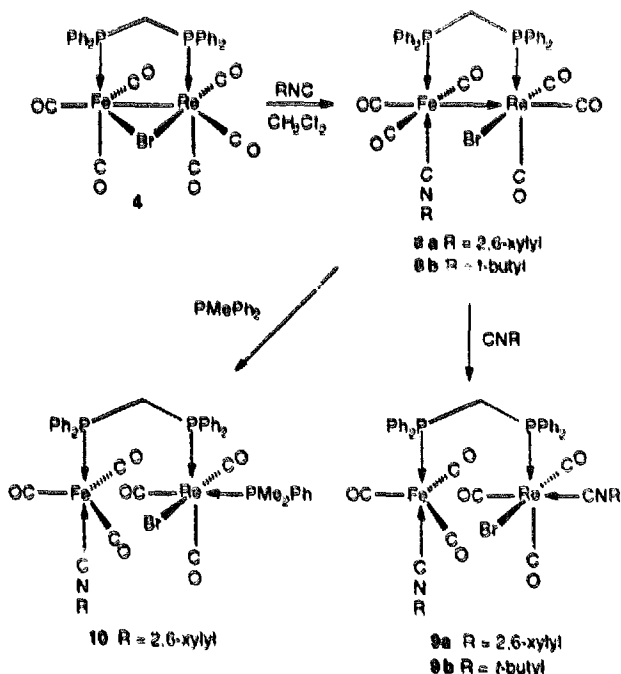


This off-white complex appears to be labile, since after repeated attempts at recrystallization only *fac*- $[\text{Re}(\text{Br})(\text{CO})_3(\text{dppm}-P,P)]$ ($^{31}\text{P}\{^1\text{H}\}$ NMR (C_6D_6 /toluene): δ -36.7, lit. value -38.5 [27]; $\nu(\text{CO})$ (KBr): 2025 vs, 1943 s, 1905 s; FIR (polyethylene) $\nu(\text{Re}-\text{Br})$: 198 cm^{-1}) could be isolated.

2.1.3. Reactions with isonitriles

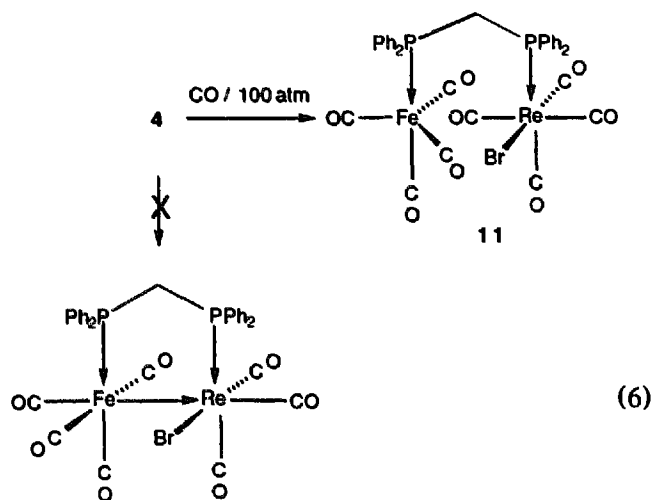
In contrast to the phosphine reactions described above, the stoichiometric addition of isonitriles to **4** afforded the yellow complexes $[(\text{OC})_3(\text{RNC})\text{Fe}(\mu\text{-dppm})\text{ReBr}(\text{CO})_3]$ (**8**) (Scheme 1). In the presence of a second equivalent of isonitrile, the dative Fe-Re bond was cleaved to give, in excellent yield, the yellow isonitrile adducts $[(\text{OC})_3(\text{RNC})\text{Fe}(\mu\text{-dppm})\text{ReBr}(\text{CNR})(\text{CO})_3]$ (**9**), which are probably structurally analogous to the phosphine derivatives **5**. The cleavage of the metal-metal bond is manifested in the magnitude of the $J(\text{P}-\text{P})$ coupling, which is reduced in the case of **8b** from 71 to 32 Hz after the transformation to **9b**.

In a similar manner, the mixed phosphine, isonitrile complex **10** containing a xylyl-isonitrile ligand on iron and a phosphine ligand on rhenium was isolated after addition of PMePh_2 to **8a**. Bubbling of CO through a solution of **4** for 40 min did not lead to spectral changes. However, when a CH_2Cl_2 solution of **4** was exposed to



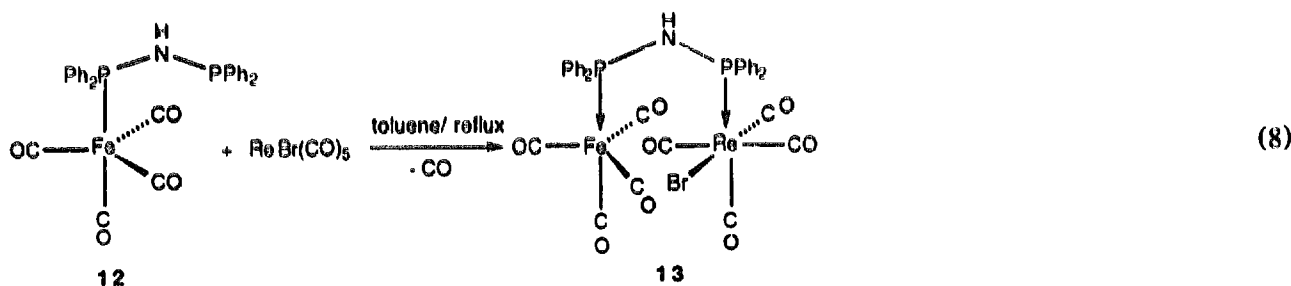
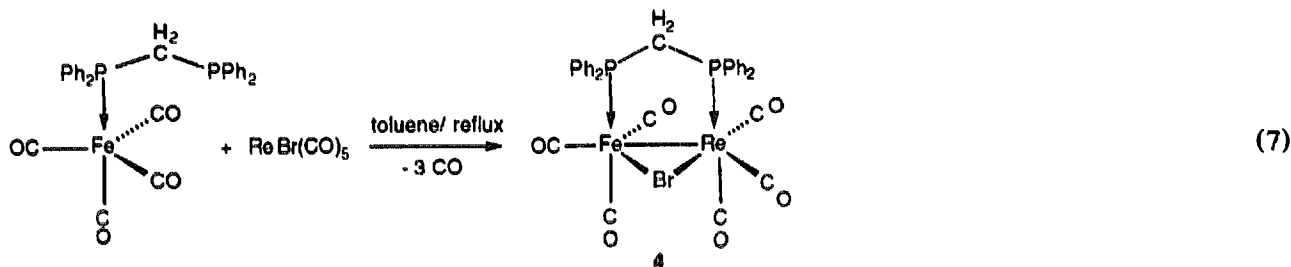
Scheme 1.

100 bar CO, a nearly quantitative conversion to $[(OC)_4Fe(\mu\text{-dppm})ReBr(CO)_4]$ (**11**) was observed (Eq. (6)).



The IR spectrum of **11** consists of the superimposition of the patterns corresponding to an $Fe(CO)_4PR_3$

and a $cis\text{-}ReBr(CO)_4PR_3$ moiety. We assign the vibration at 2053, 1982 and 1949 cm^{-1} to the iron carbonyl stretches and the four remaining vibrations at 2105, 2019, 2001 and 1937 cm^{-1} to the $Re(CO)_4$ part. This agrees well with the pattern reported for $cis\text{-}[ReBr(CO)_4(PMe_2Ph)]$ (2105, 2014, 2001 and 1941 cm^{-1}) [28]. We found no evidence for the formation of a monoadduct $[(OC)_4Fe(\mu\text{-dppm})ReBr(CO)_3]$ of the type illustrated in Eq. (6). It is interesting to note that an Mn–Fe complex containing a dative $Fe \rightarrow Mn$ bond has been prepared by Shaw's group via the reaction of $[Fe(CO)_4(dppm-P)]$ with $[Mn(\mu\text{-}Br)(CO)_4]_2$ in hot toluene [29]. This complex also reacted with CO to give $[(OC)_4Fe(\mu\text{-dppm})MnBr(CO)_4]$, which is analogous to **11**. When $[ReBr(CO)_5]$ was treated with $[Fe(CO)_4(dppm-P)]$ [29] in hot toluene, only complex **4** was isolated (Eq. (7)). Surprisingly, treatment of $[ReBr(CO)_5]$ with $[Fe(CO)_4(dppa-P)]$ (dppa = bis(diphenylphosphino)amine) (**12**) (see Section 3) in hot toluene afforded stable $[(OC)_4Fe(\mu\text{-dppa})ReBr(CO)_4]$ (**13**) (Eq. (8)), which even under prolonged heating did not lose further CO ligands to form the dppa analogue of **4**.



Complex **13** represents a rare example of a dppa-bridged heterometallic complex. The pattern of the IR spectrum in the $\nu(CO)$ region is identical to that of **11**, but shifted slightly to higher wavenumbers owing to a somewhat weaker electron donating capacity of dppa compared with dppm. The $^{31}P\{^1H\}$ NMR spectrum of **13** consists of an AX pattern, with a doublet at δ 37.8 ($^2J(P-P) = 54\text{ Hz}$) and a doublet at δ 117.1 for the Re-bound and Fe-bound P nuclei respectively. The N–H resonance appears at δ 6.22 in the 1H NMR spectrum in the form of a broad doublet (probably with additional unresolved couplings). A nearly identical chemical shift has been reported for the N–H resonance of the homo-

bimetallic complex $[(OC)_5Re(\mu\text{-dppa})Re(CO)_5][BF_4]_2$ (δ 6.20, triplet) [30].

In conclusion, we have found that reaction of $[HFe(Si(OMe)_3)(CO)_3(dppm-P)]$ with the coordinatively unsaturated rhenium complex $fac\text{-}[ReBr(CO)_3(THF)_2]$, which is formed in situ upon dissolving $fac\text{-}[Re(\mu\text{-}Br)(CO)_3(THF)_2]$ in THF, proceeds via reductive elimination of the silane and formation of a metal–metal bond. This contrasts with previous reactions involving Pd, Pt, Rh and Ru complexes, where stable, silyl-substituted heterometallic complexes were isolated. The bromide-bridged Fe–Re complex **4** is an interesting precursor for the study of the metallo-site selectivity in

reactions with nucleophiles. Thus, this complex reacts with one equivalent of two electron donor ligands such as phosphines, phosphites or isonitriles by opening of the halide bridge and selective coordination to the iron centre. Addition of a second equivalent leads to opening of the metal–metal bond rather than to displacement of a CO ligand. Comparison between dppm- and dppa-bridged complexes shows a significant influence of the CH₂ or NH spacer: the latter disfavoured formation of metal–metal bonded complexes, although dppa-bridged bimetallic complexes possessing a metal–metal bond have been reported in the literature [31–34].

3. Experimental section

All reactions were performed in Schlenk tube flasks under purified nitrogen. Solvents were dried and distilled under nitrogen before use, tetrahydrofuran over sodium benzophenone–ketyl, toluene, benzene and hexane over sodium, dichloromethane from P₂O₅. Nitrogen (Air liquide, R-grade) was passed through BASF R3-11 catalyst and molecular sieve columns to remove residual oxygen or water. Elemental C, H and N analyses were performed by the Service Central de Microanalyses du CNRS. Infrared spectra were recorded in the 4000–400 cm⁻¹ region on a Bruker IFS 66 and in the 500–90 cm⁻¹ region on a Bruker IFS113 spectrometer. The ¹H, ³¹P(¹H) and ¹³C(¹H) NMR spectra were recorded at 300, 121.5 and 75.5 MHz respectively, on a Bruker AC 300 instrument. Phosphorus chemical shifts were externally referenced to 85% H₃PO₄ in H₂O with a downfield chemical shift reported as positive. The ¹⁹F(¹H) NMR spectrum was recorded at 376.5 MHz on a Bruker AM 400 instrument and referenced to CF₃Cl. The reactions were generally monitored by IR in the ν(CO) region.

3.1. Synthesis of [(OC)₃{(MeO)₃Si}Fe(μ-dppm)Re(CO)₄] (2a)

A solution of K[Fe(CO)₃{Si(OMe)₃}(dppm-P)] (K·1) (0.685 g, 1.0 mmol) in THF (25 ml) was added to a solution of *fac*-[ReBr(CO)₃(THF)₂] (1.0 mmol) in THF (5 ml). The reaction mixture was stirred for ca. 12 h. The resulting clear orange–red solution was filtered and the solvent was removed under reduced pressure. Extraction of the residue with two portions of warm Et₂O (2 ml) and addition of hexane to the combined fractions led to the precipitation of 2a on reducing the volume under reduced pressure. The yellow product, which is air-stable for short periods of time in the solid state, was isolated in 54% yield. Anal. Found: C, 44.14; H, 3.32. C₃₅H₃₁FeO₁₀P₂ReSi (*M* = 943.71) Calc.: C, 44.54; H, 3.31%. IR (THF) ν(CO): 2084 m, 2010 s, 1988 vs, 1984 sh, 1934 m, 1921 s, 1898 m. (CH₂Cl₂): 2085 m,

2010 s, 1988 vs, 1984 sh, 1937 m, 1919 s, 1895 m cm⁻¹. ¹H NMR (C₆D₆): δ 3.82 (t, partially obscured by the Si(OMe)₃ resonance, 2H, PCH₂P, ²J(P–H) = 10 Hz), 3.84 (s, 9H, OCH₃), 6.91–7.43 (m, 20H, C₆H₅). ³¹P(¹H) NMR (C₆D₆): δ 59.6 (d, P(Fe)), 1.0 (d, P(Re), ²⁺³J(P–P) = 92 Hz). ¹³C(¹H) NMR (CDCl₃): δ 216.5 (d, 2FeCO, ²J(P–C) = 12 Hz), 212.3 (d, br, not resolved, FeCO), 193.4 (d, 2ReCO, ²J(P–C) = 9 Hz), 189.1 (dd, ReCO, ²J(P–C) = 51, ³J(P–C) = 4 Hz), 185.3 (d, 1ReCO, ²J(P–C) = 8 Hz), 128.6–135.7 (phenyl), 51.3 (s, OCH₃), 44.8 (t, PCP, ¹J(P–C) = 24 Hz).

3.2. Synthesis of [(OC)₃{(MeO)₂FSi}Fe(μ-dppm)Re(CO)₄] (3)

To a stirred solution of 2a (0.189 g, 0.2 mmol) in CH₂Cl₂ (10 ml) was added dropwise a solution of BF₃·xEt₂O (126 ml, 0.2 mmol) in CH₂Cl₂ (3 ml). The reaction mixture was stirred for ca. 1 h. The resulting clear pale yellow solution was filtered and taken to dryness under reduced pressure to remove all volatiles. Yellow, air-stable crystals were obtained (0.108 g, 58%) by layering a concentrated CH₂Cl₂ solution with hexane and keeping it at –20°C for a few days. Anal. Found: C, 44.09; H, 3.27. C₃₄H₂₈FeFO₉P₂ReSi (*M* = 931.68) Calc.: C, 43.83; H, 3.03%. IR (CH₂Cl₂) ν(CO): 2087 m, 2011 s, 1990 vs, 1942 sh, 1928 s, 1903 m cm⁻¹. ¹H NMR (C₆D₆): δ 3.78 (t, partially obscured by the Si(OMe)₂ resonance, 2H, PCH₂P, ²J(P–H) = 10 Hz), 3.81 (s, 6H, OCH₃), 6.90–7.45 (m, 20H, C₆H₅). ³¹P(¹H) NMR (C₆D₆): δ 59.0 (dd, P(Fe), ³J(P–P) = 18 Hz), 0.5 (d, P(Re), ²⁺³J(P–P) = 90 Hz). ¹⁹F(¹H) (CDCl₃): δ –96.5 (d, ³J(P–F) = 18 Hz), ¹J(Si–F) = 365 Hz). ¹³C(¹H) NMR (CDCl₃): δ 216.6 (d, 2FeCO, ²J(P–C) = 12 Hz), 211.2 (d, FeCO, ²J(P–C) = 17 Hz), 192.9 (dd, 2ReCO, ²J(P–C) = 10, ³J(P–C) = 3 Hz), 189.1 (dd, ReCO, ²J(P–C) = 53, ³J(P–C) = 6 Hz), 184.8 (d, 1ReCO, ²J(P–C) = 8 Hz), 128.6–135.5 (phenyl), 51.0 (d, OCH₃, ³J(F–C) = 4 Hz), 44.6 (t, PCP, ¹J(P–C) = 24 Hz).

3.3. Synthesis of [(OC)₃Fe(μ-Br)(μ-dppm)Re(CO)₃] (4)

To a stirred solution of [HFe(CO)₃{Si(OMe)₃}(dppm-P)](H·1) (0.653 g, 1.0 mmol) in toluene (10 ml) was added [Re(CO)₃(THF)(μ-Br)]₂ (0.422 g, 0.5 mmol). The clear orange solution was stirred for 1 h. During this period partial precipitation of the product occurred. Reduction of the solvent under reduced pressure and addition of hexane (15 ml) completed the precipitation of 4 as a yellow solid, which was filtered off, rinsed with Et₂O (4 ml), and dried in vacuo (0.831 g, 95%). Recrystallisation from toluene/hexane afforded air-stable, orange–yellow crystals of 4. Anal. Found: C, 43.46; H, 2.85. C₃₁H₂₂BrFeO₆P₂Re (*M* = 874.42) Calc.: C,

42.58; H, 2.54%. IR (CH₂Cl₂) ν (CO): 2107 vw, 2043 vs, 2009 s, 1941 m,sh, 1934 s, 1920 s cm⁻¹. ¹H NMR (C₆D₆): δ 2.37 (m, 1H, PCH), 3.21 (m, 1H, PCH), 6.63–7.39 (m, 20H, C₆H₅). ³¹P{¹H} NMR (C₆D₆/CH₂Cl₂): δ 57.2 (d, P(Fe)), 10.4 (d, P(Re)), ²⁺³J(P–P) = 80 Hz). ¹³C{¹H} (CDCl₃): δ 213.8 (d, 3FeCO, ²J(P–C) = 7 Hz), 192.2 (d, 1ReCO, ²J(P–C) = 8 Hz), 190.1 (dd, ReCO, ²J(P–C) = 69, ³J(P–C) = 3 Hz), 188.6 (d, 1ReCO, ²J(P–C) = 7 Hz), 128.6–135.7 (phenyl), 51.3 (s, OCH₃), 22.4 (t, PCP, ¹J(P–C) = 19 Hz).

3.4. Synthesis of [(OC)₃(R₃P)Fe(μ -dppm)ReBr(CO)₃(PR₃)] (5)

To a stirred solution of 4 (0.087 g, 0.1 mmol) in CH₂Cl₂ (5 ml) was added PR₃ (0.21 mmol). The clear yellow solution was stirred for 1 h. Evaporation of the solvent under reduced pressure to ca. 2 ml and addition of hexane (10 ml) induced the precipitation of 6 in the form of pale yellow solids. After completion of the precipitation at 5°C the solid was filtered and dried under vacuum to afford 6 in ca. 85–90% yield.

5a (PR₃ = P(Ph)₃). Anal. Found: C, 54.26; H, 3.56. C₆₇H₅₂BrFeO₁₂P₄Re (*M* = 1495.00) Calc.: C, 53.83; H, 3.51%. IR (CH₂Cl₂) ν (CO): 2048 s, 1976 m, 1920 s,sh, 1910 vs, 1897 s; ν (ReBr) in polyethylene: 197 cm⁻¹. ¹H NMR (C₆D₆): δ 4.64 (m, 1H, CH), 5.73 (m, 1H, CH), 6.61–8.02 (m, 50H, C₆H₅). ³¹P{¹H} NMR (acetone-*d*₆/CH₂Cl₂): δ 180.5 (d, P⁴(Fe), ²J(P⁴–P¹) = 86 Hz), 102.2 (d, P³(Re), ²J(P³–P²) = 35 Hz), 72.9 (dd, P¹(Fe), ²J(P¹–P⁴) = 86, ²⁺³J(P¹–P²) = 35 Hz), –3.1 (t, P²(Re), ²J(P²–P³) = 35, ²⁺³J(P²–P¹) = 35 Hz).

5b (PR₃ = PMePh₂). Anal. Found: C, 53.27; H, 3.67. C₅₇H₄₀BrFeO₆P₄Re (*M* = 1274.86) Calc.: C, 53.70; H, 3.79%. IR (CH₂Cl₂) ν (CO): 2033 vs, 1952 s, 1905 s, 1885 s, 1877 sh cm⁻¹. ¹H NMR (C₆D₆): δ 1.82 (d, 3H, PCH₃, ²J(P–H) = 9.1 Hz), 2.18 (d, 3H, PCH₃, ²J(P–H) = 8.2 Hz), 4.08 (m, 1H, CH), 5.35 (m, 1H, CH), 6.81–7.94 (m, 40H, C₆H₅). ³¹P{¹H} NMR (acetone-*d*₆/CH₂Cl₂): δ 77.1 (t, P¹(Fe), ²J(P¹–P⁴) = 32, ²⁺³J(P¹–P²) = 32 Hz), 65.4 (d, P⁴(Fe), ²J(P⁴–P¹) = 35), –2.6 (t, P²(Re), ²J(P²–P³) = 32, ²⁺³J(P²–P¹) = 32 Hz), –19.1 (d, P³(Re), ²J(P³–P²) = 32 Hz).

5c (PR₃ = PMe₂Ph). Anal. Found: C, 48.59; H, 3.42. C₄₇H₄₄BrFeO₆P₄Re (*M* = 1150.72) Calc.: C, 49.06; H, 3.85%. IR (CH₂Cl₂) ν (CO): 2032 vs, 1950 s, 1903 s, 1881 vs, 1875 sh cm⁻¹. ¹H NMR (C₆D₆): δ 1.47 (m, 6H, PCH₃), 1.64 (“dd”, 6H, PCH₃, ²⁺⁴J(P–H) = 5.6, 6.0 Hz), 3.94 (m, 1H, CH), 5.45 (m, 1H, CH), 6.63–7.98 (m, 30H, C₆H₅). ³¹P{¹H} NMR (acetone-*d*₆/CH₂Cl₂): δ 75.3 (t, P¹(Fe), ²J(P¹–P⁴) = 31, ²⁺³J(P¹–P²) = 31 Hz), 51.4 (d, P⁴(Fe), ²J(P⁴–P¹) = 31 Hz), –2.7 (t, P²(Re), ²J(P²–P³) = 31, ²⁺³J(P²–P¹) = 31 Hz), –34.9 (d, P³(Re), ²J(P³–P²) = 31 Hz).

3.5. Synthesis of [(OC)₃(RN≡C)Fe(μ -dppm)ReBr(CO)₃] (8)

To a solution of 4 (0.087 g, 0.1 mmol) in CH₂Cl₂ (5 ml) was added 2,6-xylylisonitrile (0.0132 g, 0.1 mmol) or ¹BuNC (12 μ l, 0.1 mmol) diluted in 3 ml of CH₂Cl₂. After completion of the reaction (10 min, IR monitoring), the clear yellow solution was evaporated to dryness and the yellowish residue washed with 2 ml hexane and then dried in vacuo to yield pure 8 in ca. 90% yield.

8a (R = 2,6-xylyl). Anal. Found: C, 47.84; H, 3.10; N, 1.44. C₄₀H₃₁BrFeNO₆P₂Re (*M* = 1005.60) Calc.: C, 47.78; H, 3.11; N, 1.39%. IR (CH₂Cl₂) ν (NC): 2149 s; ν (CO): 2034 m, 2010 vs, 1971 s, 1925 s, 1886 m cm⁻¹. ¹H NMR (C₆D₆): δ 2.20 (s, 6H, CH₃), 4.18 (m, 1H, PCH), 5.42 (m, 1H, PCH), 6.49–8.08 (m, 23H, phenyl). ³¹P{¹H} NMR (C₆D₆/CH₂Cl₂): δ 59.6 (d, P(Fe)), 7.4 (d, P(Re), ²⁺³J(P–P) = 70 Hz).

8b (R = ¹Bu). Anal. Found: C, 45.24; H, 3.47; N, 1.36. C₃₆H₃₁BrFeNO₆P₂Re (*M* = 957.55) Calc.: C, 45.16; H, 3.26; N, 1.46%. IR (CH₂Cl₂) ν (NC): 2175 m; ν (CO): 2035 m, 2008 vs, 1967 s, 1923 s, 1884 m cm⁻¹. ¹H NMR (C₆D₆): δ 0.92 (s, 9H, CH₃), 4.20 (m, 1H, PCH), 5.39 (m, 1H, PCH), 6.78–8.05 (m, 20H, C₆H₅). ³¹P{¹H} NMR (C₆D₆/CH₂Cl₂): δ 60.9 (d, P(Fe)), 7.0 (d, P(Re), ²⁺³J(P–P) = 71 Hz).

3.6. Synthesis of [(OC)₃(RN≡C)Fe(μ -dppm)ReBr(C≡NR)(CO)₃] (9)

To a solution of 4 (0.087 g, 0.1 mmol) in CH₂Cl₂ (5 ml) was added 2,6-xylylisonitrile (0.0276 g, 0.21 mmol) diluted in 3 ml of CH₂Cl₂. After completion of the reaction (15 min, IR monitoring) the clear yellow solution was evaporated to dryness and the yellowish residue washed with 2 ml hexane and then dried in vacuo to yield pure 9a (0.098 g, 86%). Bright yellow 9b was prepared in a similar manner using toluene as solvent and it was isolated in 89% yield as a toluene solvate.

9a (R = 2,6-xylyl). Anal. Found: C, 52.23; H, 3.20; N, 2.31%. C₄₉H₄₀BrFeN₂O₆P₂Re (*M* = 1136.78) Calc.: C, 51.77; H, 3.55; N, 2.46%. IR (CH₂Cl₂) ν (CN): 2162 m, 2124 s; ν (CO): 2034 vs, 1971 s, 1917 vs, 1899 sh; ν (ReBr) in polyethylene: 195 cm⁻¹. ¹H NMR (C₆D₆): δ 2.03 (s, 6H, CH₃), 2.15 (s, 6H, CH₃), 4.71 (m, 1H, PCH), 5.26 (m, 1H, PCH), 6.62–8.18 (m, 26H, phenyl). ³¹P{¹H} NMR (CDCl₃): δ 69.3 (d, P(Fe)), –1.1 (d, P(Re), ²⁺³J(P–P) = 31 Hz).

9b (R = ¹Bu). Anal. Found: C, 49.12; H, 4.78; N, 2.73. C₄₁H₄₀BrFeN₂O₆P₂Re · 0.5C₇H₈ (*M* = 957.55 + 46.03) Calc.: C, 49.0; H, 4.12; N, 2.60%. IR (CH₂Cl₂) ν (CN): 2177 s, 2145 m; ν (CO): 2034 vs, 1967 s, 1911 vs, 1885 sh; ν (ReBr) in polyethylene: 191 cm⁻¹. ¹H NMR (C₆D₆): δ 0.87 (s, 9H, CH₃), 0.94 (s, 9H, CH₃), 4.35 (m, 1H, PCH), 5.47 (m, 1H, PCH), 6.79–8.03 (m,

20H, C₆H₅). ³¹P{¹H} NMR (C₆D₆/CH₂Cl₂): δ 71.7 (d, P(Fe)), -1.2 (d, P(Re)), ²⁺³J(P-P) = 32 Hz).

3.7. Synthesis of [(OC)₃(xylyl-N≡C)Fe(μ-dppm)ReBr(CO)₃(PMePh₂)] (10)

To a stirred solution of **8a** (0.101 g, 0.1 mmol) in CH₂Cl₂ (5 ml) was added PMePh₂ (0.1 mmol). The clear yellow solution was stirred for 15 min. Reduction of the solvent under reduced pressure to ca. 2 ml and addition of hexane (10 ml) induced the precipitation of **10** as a pale yellow solid. After completion of the precipitation at 5°C, the product was filtered and dried under vacuum (0.092 g, 76%). Anal. Found: C, 53.26; H, 3.71; N, 1.05. C₅₃H₄₄BrFeNO₆P₃Re (M = 1205.82) Calc.: C, 52.79; H, 3.67; N, 1.16%. IR (CH₂Cl₂) ν(CN): 2123 m; ν(CO): 2034 vs, 1982 m, 1953 s, 1909 vs, br cm⁻¹. ¹H NMR (C₆D₆): δ 2.08 (9H, PCH₃ and xylyl-CH₃ superimposed), 4.08 (m, 1H, CH), 5.26 (m, 1H, CH), 6.59–7.70 (m, 33H, phenyl). ³¹P{¹H} NMR (C₆D₆/CH₂Cl₂): δ 72.3 (d, P¹(Fe)), ²⁺³J(P¹-P²) = 32 Hz), -2.4 (dd, P²(Re)), ²J(P²-P³) = 28, ²⁺³J(P²-P¹) = 32 Hz), -18.9 (d, P³(Re)), ²J(P³-P²) = 28 Hz).

3.8. Synthesis of [(OC)₄Fe(μ-dppm)ReBr(CO)₄] (11)

A concentrated solution of **4** (0.174 g, 0.2 mmol) in CH₂Cl₂ (3 ml) was pressurized in an autoclave under 100 bar of CO for 1 h. After removal of the solvent, the residue was extracted with warm hexane (2 × 15 ml). The combined extracts were evaporated to dryness to give the pure yellow product (0.154 g, 83%). Anal. Found: C, 42.81; H, 2.47. C₁₁H₂₂BrFeO₈P₂Re (M = 930.44) Calc.: C, 42.60; H, 3.8%. IR (CH₂Cl₂) ν(CO): 2007 w, 2050 m, 2008 sh, 2004 vs, 1977 m, 1944 vs, br; (hexane): 2105 w, 2053 s, 2019 m, 2001 vs, 1982 m, 1949 vs, 1937 cm⁻¹. ¹H NMR (CDCl₃): δ 3.48 (m, 1H, CH), 4.40 (m, 1H, CH), 7.15–7.79 (m, 20H, C₆H₅). ³¹P{¹H} NMR (CDCl₃): δ 66.2 (d, P¹(Fe)), -3.9 (d, P²(Re)), ²⁺³J(P²-P¹) = 32 Hz).

3.9. Synthesis of [Fe(CO)₄(dppa-P)] (12)

This complex was obtained in 45% yield as brown-yellow powder by the reaction of [Fe₂(CO)₉] with dppa [35] in THF as described by Shaw and coworkers [29] for [Fe(CO)₄(dppm-P)]. Anal. Found: C, 60.92; H, 3.91; N, 2.46. C₂₈H₂₁FeNO₄P₂ (M = 553.27) Calc.: C, 60.78; H, 3.83; N, 2.53%. (KBr) ν(NH): 3344 w; ν(CO): 2048 s, 1973 m, 1928 vs, br cm⁻¹. ¹H NMR (CDCl₃): δ 3.58 (s, br, 1H, NH), 7.15–7.81 (m, 20H, C₆H₅). ³¹P{¹H} NMR (CDCl₃): δ 114.9 (d, P¹(Fe)), 33.0 (d, P²(uncoord.)), ²⁺³J(P²-P¹) = 46 Hz).

3.10. Synthesis of [(OC)₄Fe(μ-dppa)ReBr(CO)₄] (13)

A mixture of [Fe(CO)₄(dppa-P)] (0.110 g, 0.2 mmol) and [ReBr(CO)₃] (0.082 g, 0.2 mmol) in toluene (10 ml)

was heated under reflux for 1 h. After filtration and concentration of the solution to ca. 2 ml, the colourless product was precipitated by addition of hexane. After completion of the precipitation at 5°C, **13** was filtered and dried under vacuum (0.134 g, 72%). Anal. Found: C, 43.41; H, 2.51; N, 1.52. C₃₂H₂₁BrFeNO₈P₂Re · 0.5C₇H₈ (M = 931.43 + 46.03) Calc.: C, 43.62; H, 2.57; N, 1.43%. IR (CH₂Cl₂) ν(CO): 2010 w, 2050 m, 2012 s, 2008 vs, 1979 m, 1947 vs, br; (KBr) ν(NH): 3165 w; ν(CO): 2010 m, 2050 s, 2022 s, 2006 s, 1975 m, 1946 vs, br, 1925 s cm⁻¹. ¹H NMR (CDCl₃): δ 6.22 (d, br, 1H, NH), 7.16–7.82 (m, 20H, C₆H₅). ³¹P{¹H} NMR (CDCl₃): δ 117.1 (d, P¹(Fe)), 37.8 (d, P²(Re)), ²⁺³J(P²-P¹) = 54 Hz).

3.11. Crystal structure determination of the complexes [(OC)₃{(MeO)₂Si}Fe(μ-dppm)Re(CO)₄] (2a) and [(OC)₃Fe(μ-Br)(μ-dppm)Re(CO)₃] · 0.5CH₂Cl₂ (4 · 0.5CH₂Cl₂)

Crystals of **2a** suitable for X-ray analysis were obtained from THF/Et₂O/hexane solutions. All crystals of **4**, obtained from CH₂Cl₂/hexane solutions, were of poor quality, so that accurate structural results could not be obtained.

Crystal data for **2a**: C₃₅H₃₁FeO₁₀P₂ReSi, M = 943.71, triclinic, space group P1, a = 17.960(4), b = 10.736(5), c = 10.575(2) Å, α = 71.39(2), β = 105.99(2), γ = 99.16(2)°, U = 1852(1) Å³, λ = 0.71073 Å, Z = 2, D_c = 1.692 g cm⁻³, F(000) = 932, μ(Mo Kα) = 38.30 cm⁻¹.

Crystal data for **4 · 0.5CH₂Cl₂**: C₁₁H₂₂BrFeO₈P₂Re · 0.5CH₂Cl₂, M = 916.88, monoclinic, space group C2/c, a = 31.998(5), b = 12.436(3), c = 22.110(4) Å, β = 129.49(2)°, U = 6790(3) Å³, λ = 0.71073 Å, Z = 8, D_c = 1.794 g cm⁻³, F(000) = 3544, μ(Mo Kα) = 53.80 cm⁻¹.

Data were collected at room temperature on a Philips PW 1100 single-crystal diffractometer using the graphite-filtered Mo Kα radiation and the θ/2θ scan model. All reflections with θ in the range 3–30° (**2a**) were measured; 11401 (**2a**) and 5381 (**4 · 0.5CH₂Cl₂**) independent reflections, 9221 (**2a**) and 2480 (**4 · 0.5CH₂Cl₂**) having I > 2σ(I) were considered observed and used in the analysis. The individual profiles have been analyzed according to Lehmann and Larsen [36]. The intensity of one standard reflection was measured after 100 reflections as a general check on crystal and instrument stability. No significant change in the measured intensities was observed during the data collection. A correction for absorption was applied [maximum and minimum values for the transmission factors were 1.000 and 0.757 (**2a**) and 1.000 and 0.842 (**4 · 0.5CH₂Cl₂**)] [37]. The structures were solved by Patterson and Fourier methods, and refined by full-matrix

least-squares first with isotropic and then with anisotropic thermal parameters in the last cycles for all the non-hydrogen atoms, except the C(10) carbon atom (found disordered and distributed in two positions of

Table 3

Fractional atomic coordinates ($\times 10^4$) and equivalent isotropic thermal parameters ($\text{\AA}^2 \times 10^4$) with e.s.d.s in parentheses for the non-hydrogen atoms of complex 2a

Atom	x	y	z	U_{eq}^a
Re	1755(1)	-7(1)	3975(1)	244(1)
Fe	3120(1)	1273(1)	2763(1)	260(3)
P(1)	2003(1)	-2121(1)	3843(1)	253(5)
P(2)	2933(1)	-360(1)	1789(1)	239(5)
Si	3471(1)	2875(1)	3879(2)	394(7)
O(1)	2846(2)	-571(4)	6901(4)	539(19)
O(2)	1416(3)	2580(4)	4332(4)	639(21)
O(3)	418(2)	-1428(4)	5266(4)	611(21)
O(4)	665(2)	676(4)	1035(4)	585(20)
O(5)	4073(2)	-238(3)	5329(4)	435(17)
O(6)	4263(3)	2677(4)	1224(5)	772(26)
O(7)	1887(2)	2985(3)	1036(4)	594(20)
O(8)	3197(2)	2418(3)	5300(4)	438(17)
O(9)	3074(3)	4296(3)	3055(4)	697(23)
O(10)	4394(1)	3252(5)	4118(5)	1200(36)
C(1)	2474(3)	-356(5)	5832(5)	335(23)
C(2)	1555(3)	1635(5)	4180(5)	382(23)
C(3)	936(3)	-883(5)	4770(5)	379(24)
C(4)	1063(3)	411(5)	2062(6)	377(23)
C(5)	3676(3)	348(4)	4337(5)	309(21)
C(6)	3817(3)	2100(5)	1856(6)	436(26)
C(7)	2331(3)	2258(5)	1754(6)	392(24)
C(8)	3217(4)	3296(5)	6110(6)	668(34)
C(9)	3286(5)	5215(6)	1882(7)	1124(52)
C(10A)	4947(3)	2304(9)	4409(35)	3088(174)
C(10B)	4825(3)	3950(17)	5082(14)	1464(82)
C(11)	2756(3)	-1987(4)	2947(4)	268(19)
C(12)	2180(3)	-229(5)	228(5)	318(20)
C(13)	2143(4)	1024(5)	-771(5)	491(27)
C(14)	1578(4)	1166(7)	-2011(6)	635(32)
C(15)	1085(4)	141(8)	-2275(7)	660(36)
C(16)	1126(4)	-1080(7)	-1330(7)	627(34)
C(17)	1669(3)	-1243(5)	-71(6)	448(25)
C(18)	3768(3)	-753(4)	1349(4)	254(18)
C(19)	3690(3)	-1252(5)	269(5)	407(23)
C(20)	4307(3)	-1697(5)	66(5)	433(26)
C(21)	5018(3)	-1653(5)	928(6)	459(27)
C(22)	5120(3)	-1167(5)	2015(5)	438(25)
C(23)	4493(3)	-720(4)	2198(5)	365(22)
C(24)	1192(3)	-3076(4)	2993(5)	320(21)
C(25)	465(3)	-2642(5)	2461(6)	426(25)
C(26)	-125(3)	-3307(5)	1722(6)	532(28)
C(27)	20(4)	-4416(6)	1518(6)	630(32)
C(28)	740(4)	-4896(5)	2070(6)	585(31)
C(29)	1337(3)	-4234(5)	2818(6)	447(25)
C(30)	2334(3)	-3286(4)	5529(5)	307(20)
C(31)	1811(4)	-4114(5)	6168(6)	592(30)
C(32)	2068(5)	-4929(6)	7506(8)	936(44)
C(33)	2837(5)	-4905(6)	8176(7)	742(38)
C(34)	3345(4)	-4087(5)	7527(6)	543(28)
C(35)	3110(3)	-3290(5)	6218(6)	445(25)

^a Equivalent isotropic U defined as one third of the trace of the orthogonalized U_{ij} tensor.

Note: A and B label disordered atoms.

Table 4

Fractional atomic coordinates ($\times 10^4$) and equivalent isotropic thermal parameters ($\text{\AA}^2 \times 10^4$) with e.s.d.s in parentheses for the non-hydrogen atoms of complex 4 · 0.5CH₂Cl₂

Atom	x	y	z	U_{eq}^a
Re	5615(1)	1207(1)	-618(1)	555(5)
Fe	5972(1)	2739(3)	593(2)	689(21)
Br	5391(1)	1198(3)	338(1)	810(17)
P(1)	6410(2)	82(5)	354(3)	834(46)
P(2)	6719(2)	1793(5)	1562(3)	793(42)
O(1)	5885(8)	1472(21)	-1706(9)	2074(188)
O(2)	4587(8)	2580(12)	-1763(9)	1807(137)
O(3)	4915(6)	-722(10)	-1608(9)	1500(157)
O(4)	5009(5)	4096(12)	-437(8)	1557(132)
O(5)	6390(5)	3321(10)	-201(7)	1026(99)
O(6)	6381(7)	4400(11)	1787(8)	1646(156)
C(1)	5803(7)	1315(13)	-1266(8)	1843(89)
C(2)	4998(9)	2051(13)	-1312(10)	1616(83)
C(3)	5199(9)	15(14)	-1225(13)	1696(90)
C(4)	5402(5)	3561(13)	-17(9)	1300(67)
C(5)	6196(9)	2985(12)	59(9)	1500(84)
C(6)	6199(7)	3757(13)	1286(9)	1391(66)
C(7)	6672(8)	350(16)	1333(10)	1230(63)
C(8)	6853(7)	1724(14)	2479(10)	1071(53)
C(9)	6435(8)	1565(16)	2470(12)	1375(66)
C(10)	6481(7)	1407(16)	3166(10)	1245(56)
C(11)	6984(7)	1417(16)	3832(11)	1353(61)
C(12)	7453(9)	1547(17)	3915(13)	1542(72)
C(13)	7348(8)	1706(15)	3165(11)	1299(64)
C(14)	7362(7)	2226(15)	1832(9)	1092(52)
C(15)	7416(8)	3346(16)	1705(10)	1237(61)
C(16)	7861(8)	3645(19)	1844(10)	1371(61)
C(17)	8298(9)	2951(19)	2184(11)	1478(74)
C(18)	8282(8)	1868(18)	2349(10)	1297(63)
C(19)	7804(7)	1555(17)	2147(10)	1251(59)
C(20)	6999(7)	109(16)	426(10)	1086(53)
C(21)	7410(8)	-624(16)	892(11)	1297(62)
C(22)	7921(8)	-607(16)	1070(12)	1368(66)
C(23)	7973(9)	241(18)	680(12)	1422(69)
C(24)	7566(8)	962(17)	201(11)	1320(62)
C(25)	7112(7)	909(16)	119(10)	1238(60)
C(26)	6271(7)	-1354(16)	238(9)	1195(56)
C(27)	6190(7)	-1936(16)	691(11)	1347(68)
C(28)	6095(9)	-3034(17)	576(14)	1857(95)
C(29)	6010(8)	-3521(21)	-60(11)	1680(79)
C(30)	6086(8)	-2943(16)	-523(12)	1478(71)
C(31)	6224(8)	-1864(16)	-367(11)	1493(75)
C(1G)	0	8276(40)	2500	2600(206)
C(1G)	385(19)	8735(52)	2167(30)	2791(217)

^a Equivalent isotropic U defined as one third of the trace of the orthogonalized U_{ij} tensor.

equal occupancy factor) for 2a and except all carbon atoms for 4 · 0.5CH₂Cl₂. Molecules of CH₂Cl₂ solvent were found in the crystals of 4. The hydrogen atoms (except those of the methyl group at C(10) of 2a) were placed at their calculated positions (C–H 0.96 Å) and refined 'riding' on the corresponding carbon atoms. A weighting scheme $w = 1/\sigma^2(F_o)$ was used in the last cycles of refinements. Final R and R' values were 0.0405 and 0.0385 for 2a, 0.0740 and 0.0655 for 4 · 0.5CH₂Cl₂. The SHELX-76 and SHELXS-86 systems of

computer programs were used [38]. Atomic scattering factors, corrected for anomalous dispersion, were taken from Ref. [39]. Final atomic coordinates for the non-hydrogen atoms are given in Tables 3 and 4. All calculations were carried out on the GOULD POWERNODE 6040 of the Centro di Studio per la Strutturistica Diffratometrica del CNR, Parma.

Additional data available from the Cambridge Crystallographic Data Centre comprise H-atom coordinates, thermal parameters and remaining bond lengths and angles.

Acknowledgements

We are grateful to the CNRS and the Ministère de l'Enseignement Supérieur et de la Recherche (Paris) for financial support, the Commission of the European Communities (contract CHRX-CT93-0277) and the Deutsche Forschungsgemeinschaft for a habilitation grant to M.K.

References

- [1] P. Braunstein, in A.F. Williams, C. Floriani and A.E. Merbach (eds.), *Perspectives in Coordination Chemistry*, VCH, Weinheim, 1992, p. 67.
- [2] P. Braunstein, *New J. Chem.*, 18 (1994) 51.
- [3] P. Braunstein and J. Rosé, Catalysis and related reactions with compounds containing heteronuclear metal-metal bonds, in B.W. Abel, F.G.A. Stone and G. Wilkinson (eds.), *Comprehensive Organometallic Chemistry II*, Elsevier, Oxford, 1995, p. 351.
- [4] P. Johnston, G.J. Hutchings, L. Denner, J.C.A. Boeyens and N.J. Coville, *Organometallics*, 6 (1987) 1292.
- [5] W.L. Ingham and N.J. Coville, *Inorg. Chem.*, 31 (1992) 4084.
- [6] D. Sonnenberger and J.D. Atwood, *J. Am. Chem. Soc.*, 102 (1980) 3484.
- [7] P. Braunstein and M. Knorr, in N. Russo and D.R. Salahub (eds.), *Metal Ligand Interactions*, Kluwer Academic, Dordrecht, 1995, p. 49.
- [8] P. Braunstein and M. Knorr, in N. Auner and J. Weis (eds.), *Organosilicon Chemistry II*, VCH, Weinheim, 1996, p. 553.
- [9] P. Braunstein, M. Knorr, B.E. Villarroja and J. Fischer, *New J. Chem.*, 14 (1990) 583.
- [10] P. Braunstein, M. Knorr, E. Villarroja, A. DeCian and J. Fischer, *Organometallics*, 10 (1991) 3714.
- [11] P. Braunstein, M. Knorr, U. Schubert, M. Lanfranchi and A. Tiripicchio, *J. Chem. Soc., Dalton Trans.*, (1991) 1507.
- [12] D. Vitali and F. Calderazzo, *Gazz. Chim. Ital.*, 102 (1972) 587.
- [13] P. Johnston, C.A. Dickson, A.J. Markwell, L. Denner, J.C.A. Boeyens and N.J. Coville, *Inorg. Chim. Acta*, 144 (1988) 185.
- [14] M. Knorr and P. Braunstein, *Bull. Soc. Chim. Fr.*, 129 (1992) 663.
- [15] M. Knorr, P. Braunstein, A. Tiripicchio and F. Ugozzoli, *Organometallics*, 14 (1995) 4910.
- [16] D. Xu, H.D. Kesz and S.I. Khan, *Inorg. Chem.*, 30 (1991) 1341.
- [17] R.D. Adams, J.E. Cortopassi and J.H. Yamamoto, *Organometallics*, 12 (1993) 3036.
- [18] P. Braunstein, E. Colomer, M. Knorr, A. Tiripicchio and M. Tiripicchio-Camellini, *J. Chem. Soc., Dalton Trans.*, (1992) 903.
- [19] P. Braunstein, M. Knorr, A. Tiripicchio and M. Tiripicchio-Camellini, *Angew. Chem., Int. Ed. Engl.*, 28 (1989) 1361.
- [20] P. Braunstein, T. Faure, M. Knorr, T. Stährfeldt, A. DeCian and J. Fischer, *Gazz. Chim. Ital.*, 125 (1995) 35.
- [21] J. Chen, Y. Yu, K. Liu, G. Wu and P. Zheng, *Organometallics*, 12 (1993) 1213.
- [22] R.D. Adams and M. Huang, *Organometallics*, 14 (1995) 2887; 4535.
- [23] S.-E. Bouaoud, P. Braunstein, D. Grandjean, D. Matt and D. Nobel, *Inorg. Chem.*, 25 (1986) 3765.
- [24] E.W. Abel and G. Wilkinson, *J. Chem. Soc.*, (1959) 1501.
- [25] J. Hoyano and L.K. Peterson, *Can. J. Chem.*, 54 (1976) 2697.
- [26] P. Braunstein, M. Knorr, M. Strampfer, Y. Dusausoy, D. Bayeuil, A. DeCian, J. Fischer and P. Zanello, *J. Chem. Soc., Dalton Trans.*, (1994) 1533.
- [27] D.A. Edwards and J. Marshalsea, *J. Organomet. Chem.*, 131 (1977) 73.
- [28] A.E. Leins and N.J. Coville, *J. Organomet. Chem.*, 407 (1991) 359.
- [29] G.B. Jacobsen, B.L. Shaw and M. Thornton-Pett, *J. Chem. Soc., Dalton Trans.*, (1987) 1509.
- [30] P. Steil, U. Nagel and W. Beck, *J. Organomet. Chem.*, 366 (1989) 313.
- [31] J. Ellermann, G. Szucsanyi, K. Geibel and E. Wilhelm, *J. Organomet. Chem.*, 263 (1984) 297.
- [32] D. Pohl, J. Ellermann, F.A. Knoch, M. Moll and W. Bauer, *J. Organomet. Chem.*, 481 (1994) 259.
- [33] D.R. Derringer, P.E. Fanwick, J. Moran and R.A. Walton, *Inorg. Chem.*, 28 (1989) 1384.
- [34] R. Uson, J. Fornies, R. Navarro, M. Tomas, C. Fortuno, J.I. Cebollada and A.J. Welch, *Polyhedron*, 8 (1989) 1045.
- [35] H. Nöth and E. Fluck, *Z. Naturforsch.*, 39b (1984) 744.
- [36] M.S. Lehmann and F.K. Larsen, *Acta Crystallogr.*, A30 (1974) 580.
- [37] N. Walker and D. Stuart, *Acta Crystallogr.*, A39 (1983) 158.
- [38] G.M. Sheldrick, SHELX-76, *Program for crystal structure determination*, University of Cambridge, 1976; SHELXS-86, *Program for the solution of crystal structures*, University of Göttingen, 1986.
- [39] *International Tables for X-Ray Crystallography*, Vol. 4, Kynoch Press, Birmingham, 1974.